Inorganic Chemistry

Article

pubs.acs.org/IC

Synthesis and Characterization of Rare Earth Corrole–Phthalocyanine Heteroleptic Triple-Decker Complexes

Guifen Lu,*[,†,‡] Jing Li,[†] Sen Yan,[†] Weihua Zhu,[†] Zhongping Ou,[†] and Karl M. Kadish*[,‡]

[†]School of Chemistry and Chemical Engineering, Jiangsu University, Zhenjiang 212013, Peoples Republic of China

[‡]Department of Chemistry, University of Houston, Houston, Texas 77204-5003 United States

Supporting Information

ABSTRACT: We recently reported the first example of a europium triple-decker tetrapyrrole with mixed corrole and phthalocyanine macrocycles and have now extended the synthetic method to prepare a series of rare earth corrole–phthalocyanine heteroleptic triple-decker complexes, which are characterized by spectroscopic and electrochemical methods. The examined complexes are represented as $M_2[Pc(OC_4H_9)_8]_2[Cor(ClPh)_3]$, where Pc = phthalocyanine, Cor = corrole, and M is Pr(III), Nd(III), Sm(III), Eu(III), Gd(III), or Tb(III). The Y(III) derivative with OC_4H_9 Pc substituents was obtained in too low a yield to characterize, but for the purpose of comparison, $Y_2[Pc(OC_5H_{11})_8]_2[Cor(ClPh)_3]$ was synthesized and characterized in a similar manner. The molecular structure of $Eu_2[Pc(OC_4H_9)_8]_2[Cor(ClPh)_3]$ was determined by single-crystal X-ray diffraction and showed the corrole to be the central macrocycle of the triple-decker unit with a phthalocyanine on each end. Each triple-decker complex undergoes up to eight reversible or quasireversible one-electron oxidations and reductions with $E_{1/2}$ values being linearly related to the ionic radius of the central ions. The energy (E) of the main Q-band is also linearly related to the radius of the metal. Comparisons are made between the physicochemical properties of the newly synthesized mixed corrole–phthalocyanine complexes and previously characterized double- and triple-decker derivatives with phthalocyanine and/or porphyrin macrocycles.

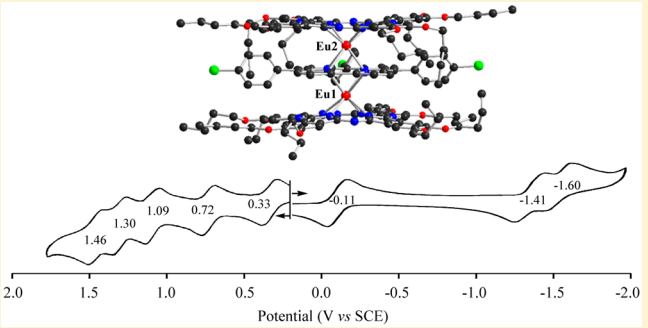

INTRODUCTION

The design and synthesis of rare earth sandwich complexes with porphyrin and/or phthalocyanine macrocycles has led to various applications of these compounds over the last two decades in the areas of sensors,[1] organic thin-film transistors,[2−4] molecular magnets,[5−13] nonlinear optical materials,[14−17] and nanomaterials.[18−20] The ongoing efforts in synthesis and characterization of new triple-decker tetrapyrroles can be attributed in large part to their remarkable optical, electrical, and electrochemical properties that stem from their intriguing inter-ring $\pi-\pi$ interactions and f–f interactions of the metal ions.[20−23] Previously synthesized triple-decker sandwich complexes with porphyrin and/or phthalocyanine macrocycles not only display a large number of redox states but also exhibit reversible electrochemistry and relatively low oxidation potentials.[21−33] For this reason, they have proven to be excellent candidates for multibit molecular information storage devices.[21−34]

Some triple-decker tetrapyrrole derivatives with mixed porphyrin and phthalocyanine macrocycles contain one porphyrin and two phthalocyanines where the porphyrin is at the central part or at the extreme end of the compound,[19,30] i.e., (Pc)M(Pc)M(Por) or (Pc)M(Por)M(Pc), while others contain two porphyrins and one phthalocyanine macrocycle where the phthalocyanine is at the center of the compound,[30] i.e., (Por)M(Pc)M(Por). The possibility of structurally modifying the arrangement of macrocycles in these types of mixed tetrapyrrole complexes provides an effective way to tune the intramolecular interactions of these complexes and to prepare specifically desired materials.[1−3,35−38] For this reason, we were interested in investigating rare earth sandwich triple-decker complexes containing mixed corrole and phthalocyanine macrocycles rather than only mixed porphyrins and phthalocyanines.

Corroles are well-characterized tetrapyrrolic macrocycles that are similar to porphyrins and phthalocyanines in many respects but contain a direct carbon–carbon bond between two pyrrole rings and carry three, rather than two, NH protons in the inner core (see Chart 1). The unique properties of corroles, and especially their metal coordination chemistry, have received a great deal of attention since the publication of improved synthetic methods by the groups of Gross, Paolesse, and Gryko in 1999.[39−42] Because corroles contain three NH protons, they possess a smaller four-nitrogen cavity than porphyrins or phthalocyanines, and they also act as trianionic ligands that exhibit both unexpected steric flexibility of the macrocycle and the ability to stabilize high oxidation states of certain

Received: March 2, 2015
Published: May 28, 2015

DOI: 10.1021/acs.inorgchem.5b00477
Inorg. Chem. 2015, 54, 5795−5805

Chart 1. Schematic Structures of Building Blocks of Sandwich Complexes

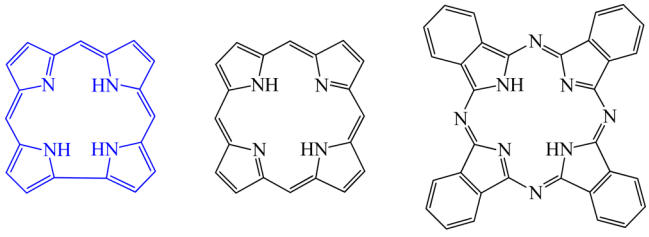

coordinated metals.[43−48] These special features of the corroles have led to a wide range of applications in the fields of catalysis, sensors, solar cells, and photodynamic therapy.[49−53]

With this in mind, we recently synthesized and structurally characterized the first example of a Eu(III) triple-decker tetrapyrrole with mixed corrole and phthalocyanine macrocycles.[54] In the present article, we have extended our synthetic method to prepare a new series of rare earth corrole−phthalocyanine heteroleptic triple-decker complexes with different metal ions and different phthalocyanine ring substituents. The examined compounds are characterized in the present paper by spectroscopic and electrochemical methods and are represented as $Y_2[Pc(OC_5H_{11})_8]_2[Cor(ClPh)_3]$ and $M_2[Pc(OC_4H_9)_8]_2[Cor(ClPh)_3]$, where Pc = phthalocyanine, Cor = corrole, and M is Pr(III), Nd(III), Sm(III), Eu(III), Gd(III), or Tb(III). The Eu(III) derivative was also structurally characterized. A detailed examination of the properties of these new sandwich complexes sheds additional light on the structural properties on this type of compound and should lead to a better understanding of the nature of triple-decker tetrapyrroles with mixed oxidation state macrocycles as well as provide useful information for future applications in the area of molecular-based information storage devices.

RESULTS AND DISCUSSION

Synthesis and Characterization. Two methods have been reported for the synthesis of rare earth heteroleptic triple-decker tetrapyrroles containing porphyrin and/or phthalocyanine macrocycles. The most commonly used synthetic method is shown in Scheme 1 as pathway a and is the so-called "one-pot" reaction with $M(acac)_3{\cdot}nH_2O$, H_2Por, and $M(Pc)_2$ as starting materials.[19,37] A second synthetic method involves the conversion of $M(acac)_3{\cdot}nH_2O$ to the "half-sandwich" M(Por)(acac), followed by addition of phthalonitriles (pathway b),[55] $M(Pc)_2$ (pathway c),[6,31,36] (Por)M(Pc) (pathway d),[36,56,57] or Li_2Pc (pathway e)[27−30,58] to give the mixed (phthalocyanine)(porphyrin) triple-decker complex as schematically illustrated in Scheme 1. The method in these syntheses is called the "raise-by-one-story" method.[21,22]

It is worth noting that pathway b, which was employed by Jiang and co-workers,[55,59,60] is an efficient way to prepare both heteroleptic bis(phthalocyanine) and mixed (phthalocyanine)(porphyrin) rare earth double-decker complexes. Pathways c and d are also equally suitable for synthesis of heterodinuclear mixed phthalocyanine or porphyrin rare earth triple-decker complexes.[55,56]

A totally different synthetic procedure is used in the present study for the preparation of the mixed corrole−phthalocyanine derivatives. This method is shown in eqs 1−3, where the target complexes **1**−**7** were obtained by prior generation of the "half-sandwich" phthalocyanine complex $M[Pc(R)_8](acac)$ from $H_2[Pc(R)_8]$[61] and the corresponding metal salt $M(acac)_3{\cdot}nH_2O$[62] in refluxing DMF (eq 1), followed by treatment with the free-base corrole $H_3[Cor(ClPh)_3]$[63] in *n*-octanol containing 1,8-diazabicyclo[5.4.0]undec-7-ene (DBU) at 170 °C (eq 2) and purified by repeated chromatography with $CHCl_3$ as eluent.

$$M(acac)_3{\cdot}nH_2O + H_2[Pc(R)_8] \xrightarrow[140\ ^\circ C]{DMF} M[Pc(R)_8](acac) + 2H(acac) \quad (1)$$

$$2M[Pc(R)_8](acac) + H_3[Cor(ClPh)_3] \xrightarrow[DBU,\ 170\ ^\circ C]{n\text{-octanol}} HM_2[Pc(R)_8]_2[Cor(ClPh)_3] + 2H(acac) \quad (2)$$

Scheme 1. Methods for the Preparation of Heteroleptic Mixed (Phthalocyaninato)(porphyrinato) Rare Earth Triple-Decker Complexes (a) by the "One-Pot" Method and (b−e) by the Stepwise Reaction Method, Where TCB = 1,2,4-Trichlorobenzene, 1-ClN = 1-Chloronaphthalene

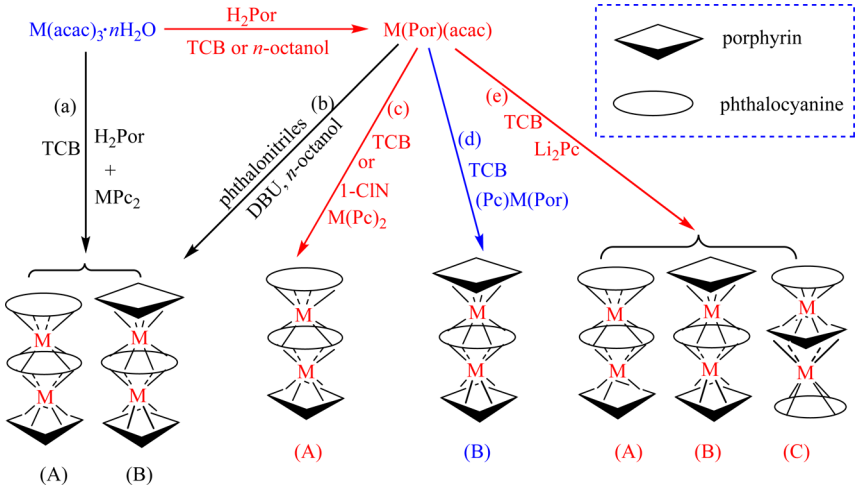

DOI: 10.1021/acs.inorgchem.5b00477
Inorg. Chem. 2015, 54, 5795−5805

$$HM_2[Pc(R)_8]_2[Cor(ClPh)_3] \overset{O_2}{\rightleftharpoons} M_2[Pc(R)_8]_2[Cor(ClPh)_3]$$

R = OC_4H_9; M = Pr (**1**), Nd (**2**), Sm (**3**), Eu (**4**), Gd (**5**), Tb (**6**) R = OC_5H_{11}; M = Y (**7**) (3)

A unique structural feature of corroles is that they have a high NH acidity relative to the NH acidity of porphyrins and phthalocyanines. Research has shown that the free base corrole, $H_3(Cor)$, when dissolved in a weakly basic solvent will often exist in its deprotonated form, $[H_2(Cor)]^-$.[64] The removal of one proton from the triprotic free base corrole, $H_3(Cor)$, can release a significant amount of energy due to steric relaxation. On this basis, the organic base DBU was selected as a promoter for the preparation of the mixed corrole−phthalocyanine rare earth triple-decker complexes **1**−**7** from the "half-sandwich" complex M[Pc(R)$_8$](acac). The yields of the final products **1**−**6** are given in the Experimental Section and range from 16% for M = Pr(III) to 31% for M = Eu(III), as compared to 15−16% for the previously synthesized Eu(III) derivatives with OC_5H_{11} and OC_8H_{17} substituents on the phthalocyanine macrocycle.[54] The yield of the compound **7** is extremely low (1%) probably because of the smaller ionic radius of the metal ion as compared to that of compounds **1**−**6**.

The relatively high yields for the preparation of complexes **1**−**6** in the present study are believed to be related to the efficiency of DBU in effectively deprotonating the corrole.[65,66] Also, the substantially higher yields for the currently investigated Eu(III) complex with OC_4H_9 phthalocyanine substituents as compared to that for the earlier reported Eu(III) derivatives with OC_5H_{11} or OC_8H_{17} groups may be related to the shorter carbon chain of substituents on the phthalocyanine macrocycle in the present study. But it should be noted that this does not hold in the case of the Y(III) derivative as mentioned above.

The final products **1**−**6** are soluble in most common organic solvents, such as $CHCl_3$ and CH_2Cl_2. They were easily purified by column chromatography, and only a small amount of the homoleptic phthalocyanine rare earth double-decker compound was obtained as a byproduct. The double-decker byproduct has a low polarity as compared to the target compounds and is easily removed from the desired target molecules. No other types of sandwich compounds (double- and triple-decker) were detected in the reaction for compounds **1**−**6**. However, an unknown byproduct was collected as a fourth band, which comes out after the target complex **7** during the purification process. The presence of the unknown byproduct may have contributed to the low yield of the target molecule.

Satisfactory elemental analyses were obtained for compounds **1**−**7** after repeated column chromatographic purification and recrystallization. Unfortunately, satisfactory ^{1}H NMR data could not be obtained. However, each newly synthesized triple-decker compound was unambiguously characterized with a wide range of spectroscopic methods, including UV−vis, IR, and MALDI-TOF mass spectrometry.

The Nature of the Complexes. All known homo- and heteroleptic triple-decker complexes with porphyrin and/or phthalocyanine macrocyles are electronically neutral, having two +3 metal ions and three −2 macrocycles (Chart 2a). This contrasts with the related double-decker complexes that can exist in two different oxidation states in their air-stable form. The majority of characterized double-decker complexes are

Chart 2. Two Forms of Rare Earth Sandwich Complexes: (a) Neutral Form and (b) Protonated Form

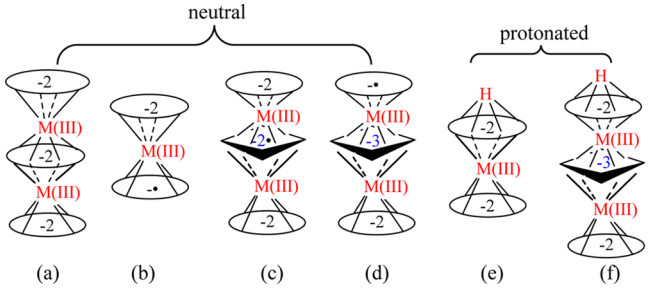

neutral and shown to possess one −2 charged macrocycle and one −1 charged radical anion macrocycle, as illustrated in Chart 2b. However, other double-decker complexes have been characterized as containing one cationic M(III) ion and two −2 charged macrocycles along with a single proton to balance the charge, as schematically shown in Chart 2e.

It should also be noted that the protonated double-decker complexes represented in Chart 2e can undergo air oxidation to give the deprotonated form shown in Chart 2b. Air oxidation to a radical form can also occur for the currently investigated corrole−phthalocyanine triple-decker complexes in Chart 2f, which formally contain two rare earth M(III) ions, one −3 corrole macrocycle and two −2 phthalocyanine macrocycles in their initial form. If air oxidation occurs as shown in eq 3, the protonated form would then gradually be converted to a neutral radical represented as $M_2(Pc^{2-})_2(Cor^{2-\bullet})$ (Chart 2c) or $M_2(Pc^{2-})(Pc^{-\bullet})(Cor^{3-})$ (Chart 2d). Both radical forms would contain one unpaired π-electron that would be delocalized over the three macrocycles. This reaction may in fact have occurred for two earlier reported mixed triple-decker compounds, which were written as $HEu_2[Pc(R)_8]_2[Cor(ClPh)_3]$,[54] where R = OC_5H_{11} or OC_8H_{17}, but upon further examination may have been converted to the radical form $Eu_2[Pc(R)_8]_2[Cor(ClPh)_3]$, as shown in the present study for seven related compounds having similar spectral and electrochemical characteristics and structures.

^{1}H NMR spectroscopy has been a powerful method to determine molecular structure and geometry in solvent. However, as mentioned above, satisfactory H NMR spectra could not be obtained for compounds **1**−**7** in d_7-DMF, d_8-THF, $CDCl_3$, or any deuterated solvent containing the reducing agent hydrazine hydrate, due either to the highly paramagnetic characteristic of the metal centers or to the presence of a radical as shown by the structures given in Chart 2c or d. Although not all of the protons on the compounds could be observed in the ^{1}H NMR spectra, a single resonance was detected in $CDCl_3$ for fresh compounds **2**−**4** in the high-field region of the spectrum. This resonance is assigned to the N−H proton of the related double-decker complexes[67−69] but in the present series of triple-decker species disappeared after a few days.

The presence of a radical such as shown in Chart 2c and d was verified by electron spin resonance (ESR) spectroscopy of the yttrium compound **7** and the appearance of the ring−ring charge transfer bands for **1**−**7** in the near-IR range of the electronic absorption spectra (discussed below). The ESR spectrum for **7** recorded in CH_2Cl_2 or as a solid at room temperature showed a characteristic organic radical signal at g = 2.002 and 2.003, respectively (see Figure S1). Both signals

DOI: 10.1021/acs.inorgchem.5b00477
Inorg. Chem. 2015, 54, 5795−5805

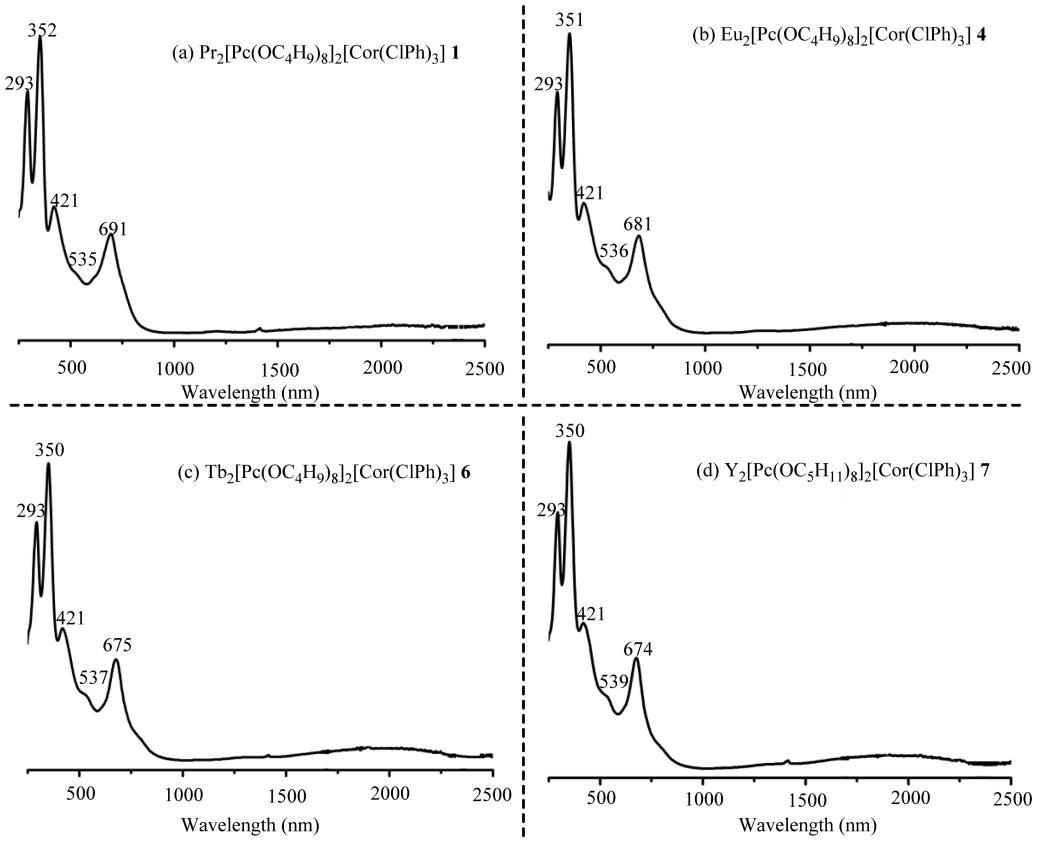

Figure 1. Electronic absorption spectra of $M_2[Pc(OC_4H_9)_8]_2[Cor(ClPh)_3]$, where M = (a) Pr **1**, (b) Eu **4**, (c) Tb **6**, and (d) $Y_2[Pc(OC_5H_{11})_8]_2[Cor(ClPh)_3]$ **7**, in CH_2Cl_2 (6.5×10^{-5} mol L^{-1}).

exhibited a narrow resolved hyperfine structure with a peak to peak separation of 6.0 and 4.0 G, respectively, thus confirming the presence of an organic radical.

Electronic Absorption Spectra. Examples of the UV−visible spectra are shown in Figure 1 for compounds **1**, **4**, **6**, and **7**, and a summary of spectral data for complexes **1**−**7** in CH_2Cl_2 are summarized in Table S1, which also includes data for the earlier reported Eu(III) derivatives.[54] As can be seen from the figure and table, the shape of the spectral envelope is similar for complexes **1**−**7**, and it is also similar to that for the previously described $Eu_2[Pc(R)_8]_2[Cor(ClPh)_3]$ derivatives where R = OC_5H_{11} or OC_8H_{17}.[54] All nine heteroleptic triple-decker complexes described in the present study exhibit a characteristic phthalocyanine N band at 293 nm,[70] a split Soret band at 350−352 and 420−421 nm, and two Q-bands at 535−539 and 674−691 nm in CH_2Cl_2. An additional broad near-IR band from 1350 to 2500 nm can also be observed for compounds **1**−**7** and is assigned to the ring−ring charge transfer band from an anion to a radical form of the macrocycles.[59,60,71] Thus, compounds **1**−**7** are described as neutral radicals, in which an unpaired electron is present on one of the three macrocyclic ligands or delocalized over all three macrocycles under the given experimental condition. These IR data described here later have bands characteristic of a −2 charge Pc macrocycle, and this would therefore favor the formulation of compound with a −2 charge Cor macrocycle.

Four of the five UV−visible bands of the investigated complexes are virtually independent of the metal ion or substituents on the phthalocyanine macrocycle, and only the relatively intense Q-band varies upon going from compound **1** to compound **7**. As seen in Figure 1 and Table S1, the position of this Q-band of the structurally related compounds **1**−**6** is systematically shifted from 691 nm to 675 nm with a decrease in the ionic radius of the M(III) ion, going from 114 pm in the case of M = Pr to 104 pm for M = Tb.[72] The energies (E) of the main Q-band of compounds **1**−**6** in CH_2Cl_2 were calculated, and the values of E in eV are summarized in Table S2, which also contains the radius of the rare earth ion of each compound.

As shown in Figure 2, there is a linear correlation between the energy (E) of the main Q-band of compounds **1**−**6** in

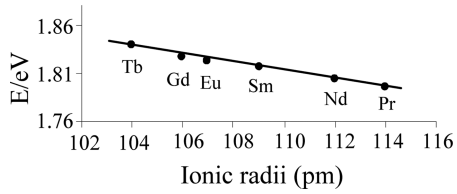

Figure 2. Correlation between the energy for the main Q-band of complexes **1**−**6** as a function of ionic radius of M^{III} (M = Pr−Tb except *Pm*) in CH_2Cl_2.

CH_2Cl_2 versus the radius of the metal ion. Compound **7** was not included in this correlation because of the different R groups on the phthalocyanine macrocycles. The values of the energy E for **1**−**6** decrease with increasing radius of the metal, thus indicating that ring−ring interactions becomes stronger as the ring−ring separation decreases; this is because of the contraction of the radius of the rare earth metal ion. A similar correlation between the NIR band of a series of lanthanoid double-decker compounds and the radius of the rare earth ion

DOI: 10.1021/acs.inorgchem.5b00477
Inorg. Chem. 2015, 54, 5795−5805

was first reported by Buchler and co-workers and was called "optical detection of the lanthanoid ion contraction".[21,72]

IR Spectra. As schematically shown in Chart 2, double- and triple-decker tetrapyrrole macrocycles can contain monoanionic radical macrocycles or dinegatively charged macrocycles. IR spectroscopy has proven to be a useful tool to distinguish these two states. As described in the literature, significant differences exist between the IR spectral signature of a dinegatively charged phthalocyanine macrocycle and a monoanionic phthalocyanine radical macrocycle in the air-stable form of the rare earth M(III) tetrapyrrolic complex.[58,59,71,73−75] For example, the double-decker compounds $Eu[Pc(R)_8]_2$ where R = OC_5H_{11} or OC_8H_{17} were shown to possess an intense band at ca. 1310−1320 cm^{-1} and a relatively weak band at ca. 1377 cm^{-1}, and on the basis of these bands one of the two macrocycles was assigned as a phthalocyanine monoanion radical.[73] In contrast, all known triple-decker phthalocyanines have a weak band at ca. 1310−1320 cm^{-1} and a strong absorption at about 1380 cm^{-1}, and in this case, the three macrocycles were assigned as phthalocyanine dianions.[73]

IR spectra of the currently investigated triple-decker complexes were also measured as KBr pellets, and the data are given in the Experimental Section. Compounds **1**−**7** all have a strong absorption at 1377−1383 cm^{-1} and a very weak band at 1307−1314 cm^{-1}. The spectra of $Eu_2[Pc(OC_4H_9)_8]_2[Cor(ClPh)_3]$ (**4**) and $Eu_2[Pc(OC_8H_{17})_8]_3$[76] also have the same pattern as shown in Figure S2, thus suggesting the dianionic nature of both phthalocyanine ligands in the mixed triple-decker complexes. This being the case, the radical form of the currently investigated complexes is proposed as $M_2(Pc^{2-})_2(Cor^{2-\bullet})$, which is shown in Chart 2c.

Two additional points should be noted. The first is that an IR characterization of corroles has rarely been given in the literature. The second is that for the currently investigated triple-deckers the phthalocyanine absorption band at 1381 cm^{-1} is less intense than that of $Eu_2[Pc(OC_8H_{17})_8]_3$, a fact that can be explained by the different number of phthalocyanine macrocycles in the two sandwich complexes, three in $Eu_2[Pc(OC_8H_{17})_8]_3$ and two in $Eu_2[Pc(OC_4H_9)_8]_2[Cor(ClPh)_3]$ (**4**).

Crystal Structure. The crystal and molecular structure of $Eu_2[Pc(OC_4H_9)_8]_2[Cor(ClPh)_3]$ (**4**) was determined by X-ray diffraction analyses. The crystal data and structure refinement are shown in Table 1. The compound crystallizes in the triclinic system with a $P\bar{1}$ space group. Two additional $CHCl_3$ solvent molecules are present in the unit cell of **4**, which is different from $Eu_2[Pc(OC_8H_{17})_8]_2[Cor(ClPh)_3]$, which contains no solvent molecules and also crystallizes in the triclinic system with a $P\bar{1}$ space group.[54]

Figure 3 displays the molecular structure of $Eu_2[Pc(OC_4H_9)_8]_2[Cor(ClPh)_3]$ (**4**) in two perspective views, with the chloroform molecules omitted for clarity. Selected bond distances and angles are given in Table S3. Each europium ion is sandwiched between an outer $Pc(OC_4H_9)_8$ ring and one central $Cor(ClPh)_3$ macrocycle. The europium centers are not identical in terms of their coordination geometry, and they are also not equidistant from the $Pc(OC_4H_9)_8$ and $Cor(ClPh)_3$ rings, as has also been described for other rare earth triple-decker tetrapyrrole compounds.[27] In the case of **4**, the Eu1 and Eu2 ions both adopt a slightly distorted square prism geometry with screw angles of 10.3° and 9.6°, respectively. Both Eu(III) ions lie closer to the outer phthalocyanine rings than to the plane of the central corrole ligand (1.342 vs 1.727 Å for Eu1

Table 1. Crystal Data and Structure Refinement of $Eu_2[Pc(OC_4H_9)_8]_2[Cor(ClPh)_3]$, 4

complex	$4{\cdot}CHCl_3$
formula	$C_{166}H_{179}Cl_6Eu_2N_{20}O_{16}$
fw	3226.91
syst	triclinic
space group	$P\bar{1}$
a (Å)	15.493(3)
b (Å)	21.656(4)
c (Å)	26.181(5)
α (deg)	69.81(3)
β (deg)	76.98(3)
γ (deg)	71.60(3)
Z	2
volume (Å^3)	7756(3)
absorp coeff (mm^{-1})	0.975
$F(000)$	3342
θ range (deg)	3 to 25
$R_1[I > 2\theta]^a$	0.0927
R_2 $[I > 2\theta]^b$	0.2604
R_{int} all	0.1115
R_{w2} all	0.2841
S	1.083

$^aR_1 = \sum||F_o| - |F_c||/\sum|F_o|$. $^bR_{w2} = [\sum w(F_o^2 - F_c^2)^2/\sum w(F_o^2)^2]^{1/2}$.

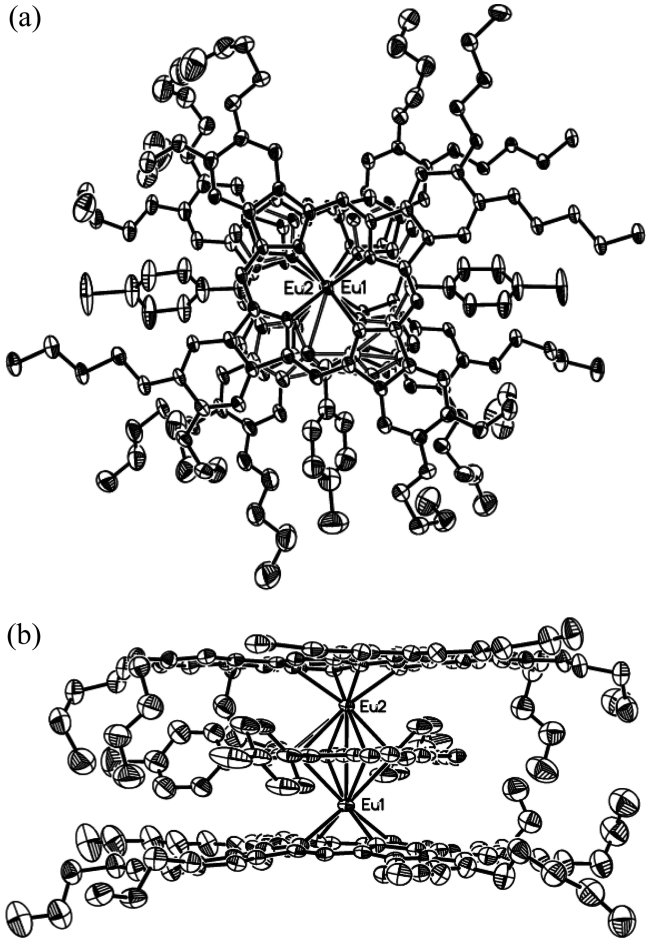

Figure 3. ORTEP drawing of molecular structure for $Eu_2[Pc(OC_4H_9)_8]_2[Cor(ClPh)_3]$ (**4**) in two perspective views: (a) top view and (b) side view (the 30% probability level). The hydrogen atoms and chloroform molecules are omitted for clarity.

DOI: 10.1021/acs.inorgchem.5b00477
Inorg. Chem. 2015, 54, 5795−5805

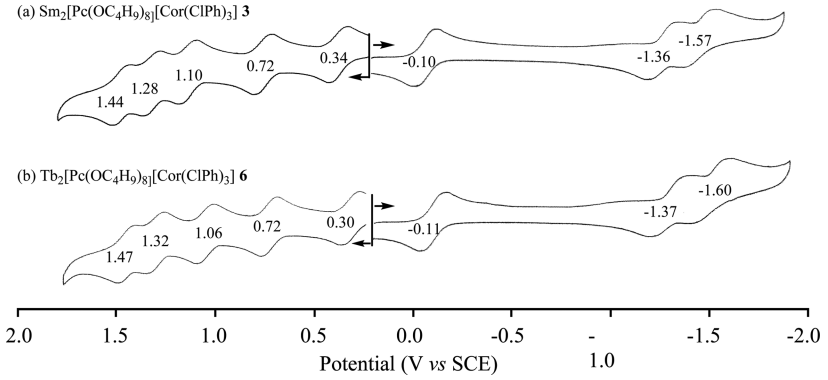

Figure 4. Cyclic voltammograms of (a) $Sm_2[Pc(OC_4H_9)_8]_2[Cor(ClPh)_3]$ (3.4×10^{-4} mol L^{-1}) and (b) $Tb_2[Pc(OC_4H_9)_8]_2[Cor(ClPh)_3]$ (3.7×10^{-4} mol L^{-1}) in CH_2Cl_2 containing 0.1 M TBAP.

Table 2. Half-Wave Potentials ($E_{1/2}$, V *vs* SCE)[a] of Complexes 1−7 in CH_2Cl_2 Containing 0.1 M TBAP[b]

Compound	oxidation					reduction			$E_{1/2}$ (Ox_1-Red_1)	$E_{1/2}$ (Red_1-Red_2)	ref
	Oxd_5	Oxd_4	Oxd_3	Oxd_2	Oxd_1	Red_1	Red_2	Red_3			
$Eu[Pc(OC_8H_{17})_8]_2$				1.33	0.36	-0.06	-1.29	-1.71	0.42	1.23	65
$Pr_2[Pc(OC_4H_9)_8]_2[Cor(ClPh)_3]$ **1**	1.51	1.30	1.14	0.71	0.41	-0.05	-1.35	-1.53	0.46	1.30	*tw*
$Nd_2[Pc(OC_4H_9)_8]_2[Cor(ClPh)_3]$ **2**	1.51	1.28	1.14	0.73	0.38	-0.06	-1.34	-1.54	0.44	1.28	*tw*
$Sm_2[Pc(OC_4H_9)_8]_2[Cor(ClPh)_3]$ **3**	1.44	1.28	1.10	0.72	0.34	-0.10	-1.36	-1.57	0.44	1.26	*tw*
$Eu_2[Pc(OC_4H_9)_8]_2[Cor(ClPh)_3]$ **4**	1.46	1.30	1.09	0.72	0.33	-0.11	-1.41	-1.60	0.44	1.30	*tw*
$Gd_2[Pc(OC_4H_9)_8]_2[Cor(ClPh)_3]$ **5**	1.48	1.32	1.08	0.73	0.32	-0.11	-1.37	-1.60	0.43	1.26	*tw*
$Tb_2[Pc(OC_4H_9)_8]_2[Cor(ClPh)_3]$ **6**	1.47	1.32	1.06	0.72	0.30	-0.11	-1.37	-1.60	0.41	1.26	*tw*
$Y_2[Pc(OC_5H_{11})_8]_2[Cor(ClPh)_3]$ **7**	1.43	1.27	0.99	0.70	0.27	-0.12	-1.29	-1.50	0.39	1.17	*tw*
$Eu_2[Pc(OC_5H_{11})_8]_2[Cor(ClPh)_3]$	1.39	1.25	1.05	0.70	0.33	-0.08	-1.27	-1.45	0.41	1.19	46
$Eu_2[Pc(OC_8H_{17})_8]_2[Cor(ClPh)_3]$	1.37	1.25	1.06	0.72	0.34	-0.09	-1.29	-1.51	0.43	1.20	46
$Eu_2[Pc(OC_8H_{17})_8]_2[Pc]$	1.45	1.30	1.14	0.63	0.26	-0.72	-1.10	-1.41			17

[a]Half-wave potential (V vs SCE) of the ferrocene/ferrocenium couple, Fe^+/Fe, is 0.48 V in CH_2Cl_2 containing 0.1 M TBAP. [b]The similarities in potentials between the newly synthesized triple-deckers and reference double- and triple-decker europium complexes are highlighted in the table. *tw* = this work.

and 1.361 vs 1.803 Å for Eu2). Interestingly, the N−Eu distances are not equivalent for the two metal ions. The average Eu1−N[$Pc(OC_4H_9)_8$] bond length (2.390 Å) is significantly shorter than the average Eu1−N[$Cor(ClPh)_3$] bond length (2.578 Å), and the Eu2−N[$Pc(OC_4H_9)_8$] (2.389 Å) distance is also shorter than the Eu2−N[$Cor(ClPh)_3$] distance (2.593 Å). This is because the central $Cor(ClPh)_3$ macrocycle is shared by two europium ions, while the outer $Pc(OC_4H_9)_8$ rings are bound to only a singel metal ion. The same was reported for the molecular structure of $Eu_2[Pc(OC_8H_{17})_8]_2[Cor(ClPh)_3]$.[54]

Table S4 lists the structural parameters of $Eu_2[Pc(OC_4H_9)_8]_2[Cor(ClPh)_3]$ (**4**), many of which are comparable with those of $Eu_2[Pc(OC_8H_{17})_8]_2[Cor(ClPh)_3]$, which has different R groups on the phthalocyanine macrocycles.[54] As shown in Table S4, the metal-to-metal distance between the two europium atoms in the $Eu_2[Pc(OC_4H_9)_8]_2[Cor(ClPh)_3]$ (**4**) molecule changes from 3.586 to 3.574 Å, when the OC_4H_9 phthalocyanine substituents in **4** are replaced by OC_8H_{17} in $Eu_2[Pc(OC_8H_{17})_8]_2[Cor(ClPh)_3]$, while the average dihedral angles between the individual isoindole ring with respect to the N4 mean plane of the corresponding phthalocyanine ring change from 5.4° to 8.6° with changes of the substituents. Both molecular structures show the corrole to be the central macrocycle of the triple-decker unit with a phthalocyanine on each end. The inner corrole ring is almost planar in $Eu_2[Pc(OC_4H_9)_8]_2[Cor(ClPh)_3]$ (**4**) and $Eu_2[Pc(OC_8H_{17})_8]_2[Cor(ClPh)_3]$,[54] with the average dihedral angle of the individual pyrrole rings being φ = 2.0° and 1.7°, respectively, with respect to the corresponding N4 mean plane.

Electrochemical Properties. The electrochemical behavior of the newly synthesized triple-decker complexes **1**−**7** was investigated by cyclic voltammetry in CH_2Cl_2 containing 0.1 M tetra-*n*-butylammonium perchlorate (TBAP). Cyclic voltammograms are shown in Figures 4 and S3−5, and the measured half-wave potentials are listed in Table 2, which also includes potentials for two related europium double-decker and triple-decker complexes under the same solution conditions.

Each compound exhibits up to five one-electron oxidations and three one-electron reductions, all of which can be attributed to ligand-based redox processes. A comparison of

DOI: 10.1021/acs.inorgchem.5b00477
Inorg. Chem. 2015, 54, 5795−5805

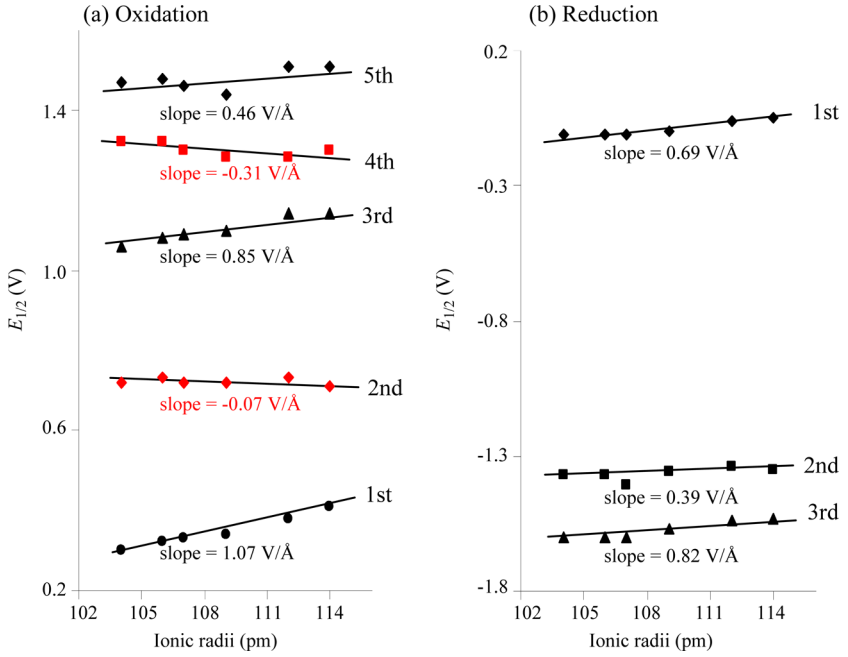

Figure 5. Half-wave potentials of redox processes of $M_2[Pc(OC_4H_9)_8]_2[Cor(ClPh)_3]$ as a function of the ionic radius of M^{III} (M = Pr−Tb, except *Pm*) in CH_2Cl_2 containing 0.1 M TBAP.

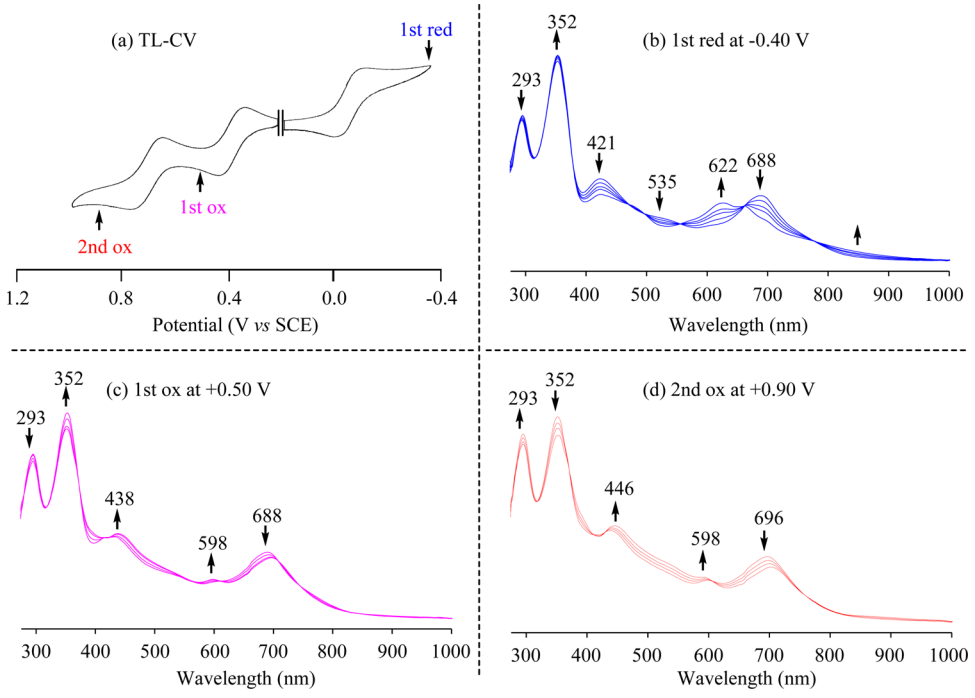

Figure 6. (a) Thin-layer cyclic voltammogram of $Nd_2[Pc(OC_4H_9)_8]_2[Cor(ClPh)_3]$ (**2**) (5.0×10^{-5} mol L^{-1}) and its UV−vis spectral changes during controlled potential reduction (b) at −0.40 V and oxidations (c) at 0.50 and (d) at 0.90 V in CH_2Cl_2 containing 0.1 M TBAP.

$E_{1/2}$ values for **1**−**7** with potentials for oxidation and reduction of related double- and triple-decker europium phthalocyanines is given in Table 2. As seen in the table, the $E_{1/2}$ values for the first oxidation and the first two reductions of **1**−**7** are virtually identical to $E_{1/2}$ values for the same redox processes of the double-decker $Eu[Pc(OC_8H_{17})_8]_2$.[77] At the same time, the second, third, fourth, and fifth oxidations of **1**−**7** are quite similar to $E_{1/2}$ values for the second to fifth oxidations of the triple-decker phthalocyanine $Eu_2[Pc(OC_8H_{17})_8]_2[Pc]$.[25] It should be noted that the difference in $E_{1/2}$ values between the first oxidation and first reduction of the newly synthesized triple-decker complexes and the double-decker reference complex $Eu[Pc(OC_8H_{17})_8]_2$ spans a relatively narrow range of potentials, 0.39−0.46 V, which accords well with previously reported data for lanthanide(III) double-decker phthalocyanine complexes.[77] It should also be noted that a similar separation in $E_{1/2}$ values is also seen between the first and second reductions of **1**−**7** and the double-decker $Eu[Pc(OC_8H_{17})_8]_2$; these values are listed as $E_{1/2}(Red_1-Red_2)$ in Table 2 and range from 1.17 to 1.30 V.

DOI: 10.1021/acs.inorgchem.5b00477
Inorg. Chem. 2015, 54, 5795−5805

The lanthanoid ion contraction in the presently investigated compounds can be seen in the redox potentials for oxidation or reduction. As shown in Figure 5, all the measured half-wave potentials (five oxidations and three reductions) for the structurally related compounds **1**−**6** correlate linearly with increasing radius of the rare earth ion. The trends of the second and fourth oxidations differ from trends of the other oxidations and reductions, which shift in the anodic direction with increasing ionic radius of the rare earth metal ion. Hence, the potentials are dependent on the ring to ring interseparations, indicating that $\pi-\pi$ interactions are also present in the heteroleptic sandwich derivatives **1**−**6**. The illustrated correlation between redox potentials and rare earth ionic radius shown in Figure 5 is similar to what has been reported in the literature for other series of rare earth sandwich tetrapyrrole complexes.[21] The trend of the redox potentials between compound **7** and $Eu_2[Pc(OC_5H_{11})_8]_2[Cor(ClPh)_3]$, which have the same macrocycles but different central metal ions, also fits this correlation.

Spectroelectrochemical Properties. The first reduction and first two oxidations of compound **1**−**6** were investigated by thin-layer UV−visible spectroelectrochemistry in CH_2Cl_2 containing 0.1 M TBAP as supporting electrolyte, and a summary of spectral data for the reduction and oxidation products is given in Table S5.

A thin-layer cyclic voltammogram is shown in Figure 6a, and examples of the spectral changes that result during controlled potential reduction and oxidations of $Nd_2[Pc(OC_4H_9)_8]_2[Cor(ClPh)_3]$ (**2**) are illustrated in Figure 6b−d. Upon the first controlled potential reduction at −0.40 V, the bands of the neutral **2** (293, 352, 421, 535, and 688 nm) decrease in intensity, while a low-intensity band at 485 nm and a sharp visible band at 622 nm grow in (Figure 6b). This reduction is reversible, and the spectrum of the neutral compound was recovered when the applied potential was set at +0.20 V.

The spectral changes obtained during the first and second oxidations at controlled potential oxidations of +0.50 and +0.90 V are illustrated in Figure 6c and d. During the first one-electron abstraction (Figure 6c), a new band at 598 nm appears and the typical phthalocyanine N band at 293 nm increases slightly as the Soret band at 351 nm slightly decreases in intensity. After the abstraction of two electrons, the relative intensity of phthalocyanine N band is almost equal to that of the Soret band (Figure 6d). The initial bands at 421 and 688 nm red-shift to 438 and 696 nm during the first oxidation (Figure 6c) and then further red-shift to 446 and 706 nm during the second oxidation (Figure 6d). Since the oxidation state of the central tervalent rare earth ions in triple-decker complexes does not change,[21,25] these redox processes are attributed to the successive removal of electrons from the ligand-based orbitals of the compound. The stepwise oxidation products in the thin-layer cell are assigned as the cation $\{Nd_2[Pc(OC_4H_9)_8]_2[Cor(ClPh)_3]\}^+$ and the dication $\{Nd_2[Pc(OC_4H_9)_8]_2[Cor(ClPh)_3]\}^{2+}$.

The first two oxidations of **2** are also reversible, and the initial spectrum could again be retrieved in the thin-layer cell by the application of a controlled reducing potential. These results confirm that the compounds in their +1 and +2 oxidation states are stable on the time scale of spectroelectrochemisty and that no chemical reactions are coupled with the electron transfer process. There is also no evidence for coupled chemical reactions involving the other redox processes, and the overall mechanism for oxidations and reductions is given in Scheme S1.

Fluorescence Properties. The currently investigated triple-decker complexes were also examined as to their fluorescence properties in CH_2Cl_2 at room temperature. However, none of the compounds were fluorescent, probably due to fast electron transfer between the face-to-face stacked tetrapyrrole rings, which is a common property of radical double-decker complexes having porphyrin and/or phthalocyanine macrocyles.[15]

CONCLUSION

In summary, a series of novel rare earth heteroleptic triple-decker tetrapyrroles with mixed corrole and phthalocyanine macrocycles were synthesized and characterized by electrochemical and spectroelectrochemical techniques. X-ray diffraction analysis confirms the corrole to be in the middle of the sandwich, with a phthalocyanine macrocycle on each extreme. The preparation of this series of triple-decker complexes provides the opportunity for exploration of new structures and fully enriches the "periodic table of corrole complexes". In particular, compounds **1**−**3** and **7** represent the first investigated Pr-, Nd-, Sm-, and Y-corrole complexes, respectively. The observation of up to five cationic states for each triple-decker complex supports the proposal of Lindsey[28−33] that this type of complex are potential molecular materials for information storage devices. In order to explore the functionalities of this type of complex, further studies about other properties, such as magnetic and nonlinear optical properties are in progress.

EXPERIMENTAL SECTION

Materials. *n*-Octanol was distilled from sodium under reduced pressure prior to use. All other reagents and solvents were purchased from Sinopharm Chemical Reagent Co. or Aldrich Chemical Co. and used as received. The compounds $H_2[Pc(OC_4H_9)_8]$,[61] $M(acac)_3 \cdot nH_2O$,[62] and $H_3[Cor(ClPh)_3]$[63] were prepared according to the literature methods.

Physical Measurements. IR spectra (KBr pellets) were recorded on an AVATAR-370 spectrometer. ^{1}HNMR spectra were recorded in a $CDCl_3$ solution at 400 MHz using a Bruker Advance 400 spectrometer at 25 °C. Chemical shifts (ppm) were determined with TMS as the internal reference. MALDI-TOF mass spectra were carried out on a Bruker BIFLEX III ultra-high-resolution Fourier transform ion cyclotron resonance (FT-ICR) mass spectrometer with α-cyano-4-hydroxycinnamic acid as matrix. Elemental analyses were performed on a FLASH1112A element analyzer. The fluorescence spectrum was recorded on a CaryEclipse fluoresence spectrophotometer. Electron spin resonance spectra were recorded in CH_2Cl_2 or as a solid at room temperature on a Bruker A300 spectrometer.

Electrochemical and Spectroelectrochemical Measurements. Absolute dichloromethane (CH_2Cl_2, 99.8%, EMD Chemicals Inc.) was used for electrochemistry without further purification. Tetra-*n*-butylammonium perchlorate, used as a supporting electrolyte, was purchased from Sigma-Aldrich, recrystallized from ethyl alcohol, and dried under vacuum at 40 °C for at least 1 week prior to use.

Cyclic voltammetry was carried out at 298 K using a CHI-730C electrochemical workstation. A homemade three-electrode cell was used for cyclic voltammetric measurements and consisted of a glassy carbon working electrode, a platinum counter electrode, and a homemade saturated calomel reference electrode (SCE). The SCE was separated from the bulk of the solution by a fritted glass bridge of low porosity, which contained the solvent/supporting electrolyte mixture. All potentials are referenced to the SCE. High-purity N_2 was used to deoxygenate the solution, and a stream of nitrogen gas was kept over the solution during each electrochemical experiment.

DOI: 10.1021/acs.inorgchem.5b00477
Inorg. Chem. 2015, 54, 5795−5805

Thin-layer UV−visible spectroelectrochemical experiments were performed with a home-built thin-layer cell that has a light transparent platinum net working electrode. Potentials were applied and monitored with an EG&G model 173 potentiostat. Time-resolved UV−visible spectra were recorded with a Hewlett-Packard model 8453 diode array spectrophotometer. High-purity N_2 from Trigas was used to deoxygenate the solution and kept over the solution during each electrochemical and spectroelectrochemical experiment.

X-ray Crystallography. Single crystals of **4** suitable for X-ray diffraction analysis were obtained by diffusion of methanol onto a solution of the corresponding compound in chloroform. Crystal data and details of data collection and structure refinement for **4** are given in Table 1. Data were collected on a Rigaku Saturn 724+ CCD X-ray diffractometer by using monochromated Mo Kα radiation (λ = 0.710 70 Å) at 120 K. Final unit cell parameters were derived by global refinements and reflections obtained from integration of all the frame data. The collected frames were integrated by using the preliminary cell-orientation matrix. CrysAlisProAgilent Technologies software was used for collecting frames of data, indexing reflections, and determination of lattice constants; CrysAlisPro Agilent Technologies for integration of intensity of reflections and scaling; and SCALE3 ABSPACK for absorption correction. The structures were solved by the direct method (SHELXS-97) and refined by full-matrix least-squares (SHELXL-97) on F^2.[65] Anisotropic thermal parameters were used for the non-hydrogen atoms, and isotropic parameters for the hydrogen atoms. Hydrogen atoms were added geometrically and refined using a riding model. The "squeeze" command was used to deal with the disorder of the solvent and molecule moiety. CCDC 1041704 for **4**, containing the supplementary crystallographic data for this paper, can be obtained free of charge from the Cambridge Crystallographic Data Centre via www.ccdc.cam.ac.uk/data_request/cif.

General Procedure for the Preparation of Heteroleptic Triple-Deckers 1−7. Heteroleptic rare earth triple-deckers **1**−**7** were synthesized according to previously reported synthetic procedures.[54] First, a mixture of $M(acac)_3{\cdot}nH_2O$ (47 mg, ca. 0.1 mmol) and $H_2[Pc(R)_8]$ (109 mg, ca. 0.1 mmol), where R = OC_4H_9 for compound **1**−**6** and R = OC_5H_{11} for compound **7**, in DMF (3 mL) was heated at 140 °C under a slow stream of nitrogen. The progress of the reaction was monitored by UV−vis spectroscopy and TLC. After the complete disappearance of starting material (ca. 1 h), the solution was cooled to room temperature, and the solvent was evaporated to give the monomeric rare earth phthalocyanine complex $M[Pc(R)_8](acac)$. This was then added to $H_3[Cor(ClPh)_3]$ (63 mg, 0.1 mmol), which was dissolved in *n*-octanol (4 mL) and heated to 170 °C for 2 h in the presence of 1,8-diazabicyclo[5.4.0]undec-7-ene (20 mg, 0.13 mmol) under a slow stream of nitrogen. The resulting green solution was cooled to room temperature, and the volatiles were removed under vacuum. The residue was chromatographed with $CHCl_3$ as eluent. A small amount of unreacted $H_3[Cor(ClPh)_3]$ and the homoleptic bis(phthalocyanine) rare earth (III) complex $M[Pc(R)_8]_2$ were collected as the first and second fractions, respectively. The target mixed ring triple-decker products were obtained as the third fraction. Repeated chromatography followed by recrystallization from $CHCl_3$ and CH_3OH gave pure $M_2[Pc(R)_8]_2[Cor(ClPh)_3]$ as gray-green solids.

*$Pr_2[Pc(OC_4H_9)_8]_2[Cor(ClPh)_3]$ (**1**).* Yield: ca. 25 mg (16%). MALDI-TOF mass: calcd 3087.493, found 3087.839. Anal. Calcd (%) for $Pr_2C_{165}H_{180}N_{20}O_{16}Cl_3$ ($CHCl_3$): C 62.17, H 5.69, N 8.74. Found: C 61.56, H 5.92, N 9.07. Main IR band (cm^{-1}): 1377 (s).

*$Nd_2[Pc(OC_4H_9)_8]_2[Cor(ClPh)_3]$ (**2**).* Yield: ca. 39 mg (26%). ^1H NMR (400 MHz, $CDCl_3$): δ 3.66 (s, 16 H, OCH_2), 2.74 (s, 16 H, OCH_2), 1.20 (t, 32 H, CH_2), 0.96 (m, 32 H, CH_2), 0.52 (t, 48 H, CH_3), −2.93 (b, 1 H, H). MALDI-TOF mass: calcd 3094.158, found 3092.997. Anal. Calcd (%) for $Nd_2C_{165}H_{180}N_{20}O_{16}Cl_3$ ($CHCl_3$): C 62.04, H 5.68, N 8.72. Found: C 61.87, H 6.12, N 8.36. Main IR bands (cm^{-1}): 1307 (w), 1383 (s).

*$Sm_2[Pc(OC_4H_9)_8]_2[Cor(ClPh)_3]$ (**3**).* Yield: ca. 35 mg (23%). ^1H NMR (400 MHz, $CDCl_3$): δ 4.21 (s, 16 H, OCH_2), 3.93 (s, 16 H, OCH_2), 1.81 (t, 32 H, CH_2), 1.50 (m, 32 H, CH_2), 0.96 (t, 48 H, CH_3), −2.39 (b, 1 H, H). MALDI-TOF mass: calcd 3106.398, found 3106.846. Anal. Calcd (%) for $Sm_2C_{165}H_{180}N_{20}O_{16}Cl_3$ (1/2$CHCl_3$): C 62.78, H 5.75, N 8.85. Found: C 62.96, H 6.21, N 8.58. Main IR bands (cm^{-1}): 1313 (w), 1381 (s).

*$Eu_2[Pc(OC_4H_9)_8]_2[Cor(ClPh)_3]$ (**4**).* Yield: ca. 48 mg (31%). ^1H NMR (400 MHz, $CDCl_3$): δ 5.38 (s, 16 H, OCH_2), 4.89 (s, 16 H, OCH_2), 2.54 (t, 32 H, CH_2), 2.17 (m, 32 H, CH_2), 1.48 (t, 48 H, CH_3), −1.35 (b, 1 H, H). MALDI-TOF mass: calcd 3109.606, found 3108.338. Anal. Calcd (%) for $Eu_2C_{165}H_{180}N_{20}O_{16}Cl_3$ (1/2$CHCl_3$): C 62.72, H 5.74, N 8.84. Found: C 62.59, H 5.74, N 9.06. Main IR bands (cm^{-1}): 1311 (w), 1381 (s).

*$Gd_2[Pc(OC_4H_9)_8]_2[Cor(ClPh)_3]$ (**5**).* Yield: ca. 43 mg (28%). MALDI-TOF mass: calcd 3120.178, found 3119.948. Anal. Calcd (%) for $Gd_2C_{165}H_{180}N_{20}O_{16}Cl_3$: C 63.73, H 5.83, N 9.01. Found: C 63.55, H 6.24, N 8.88. Main IR bands (cm^{-1}): 1314 (w), 1383 (s).

*$Tb_2[Pc(OC_4H_9)_8]_2[Cor(ClPh)_3]$ (**6**).* Yield: ca. 44 mg (28%). MALDI-TOF mass: calcd 3123.529, found 3123.351. Anal. Calcd (%) for $Tb_2C_{165}H_{180}N_{20}O_{16}Cl_3$: C 63.45, H 5.81, N 8.97. Found: C 62.96, H 6.16, N 8.55. Main IR bands (cm^{-1}): 1314 (w), 1380 (s).

*$Y_2[Pc(OC_5H_{11})_8]_2[Cor(ClPh)_3]$ (**7**).* Yield: ca. 2 mg (1%). MALDI-TOF mass: calcd 3207.915, found 3204.598. Anal. Calcd (%) for $Y_2C_{181}H_{212}N_{20}O_{16}Cl_3$: C 67.64, H 6.69, N 8.76. Found: C 67.82, H 6.57, N 8.74. Main IR bands (cm^{-1}): 1318 (w), 1380 (s).

■ ASSOCIATED CONTENT

Ⓢ Supporting Information

IR spectra, cyclic voltammograms, proposed redox mechanism, MALDI-TOF mass spectra, ^1H NMR and $^1H-^1H$ COSY spectra in $CDCl_3$, electronic absorption data, CIF file giving crystallographic data for $Eu_2[Pc(OC_4H_9)_8]_2[Cor(ClPh)_3]$, selected bond distances and angles. The Supporting Information is available free of charge on the ACS Publications website at DOI: 10.1021/acs.inorgchem.5b00477.

■ AUTHOR INFORMATION

Corresponding Authors

*E-mail: luguifen@ujs.edu.cn.

*E-mail: kkadish@uh.edu.

Notes

The authors declare no competing financial interest.

■ ACKNOWLEDGMENTS

We gratefully acknowledge support from the National Natural Science Foundation of China (Nos. 21001054, 21071067, 21171076), the Scientific Innovation Research of College Graduate in Jiangsu Province (SJLX_0482), and the Robert A. Welch Foundation (K.M.K., Grant E-680). We also thank China Council Scholarship for support.

■ REFERENCES

(1) Gao, J.; Lu, G.; Kan, J.; Chen, Y.; Bouvet, M. *Sens. Actuators, B* **2012**, *166*−*167*, 500−507.

(2) Chen, Y.; Su, W.; Bai, M.; Jiang, J.; Li, X.; Liu, Y.; Wang, L.; Wang, S. *J. Am. Chem. Soc.* **2005**, *127*, 15700−15701.

(3) Kan, J.; Chen, Y.; Qi, D.; Liu, Y.; Jiang, J. *Adv. Mater.* **2012**, *24*, 1755−1758.

(4) Kong, X.; Zhang, X.; Gao, D.; Qi, D.; Chen, Y.; Jiang, J. *Chem. Sci.* **2015**, *6*, 1967−1972.

(5) Sakaue, S.; Fuyuhiro, A.; Fukuda, T.; Ishikawa, N. *Chem. Commun.* **2012**, *48*, 5337−5339.

(6) Kan, J.; Wang, H.; Sun, W.; Cao, W.; Tao, J.; Jiang, J. *Inorg. Chem.* **2013**, *52*, 8505−8510.

(7) Morita, T.; Katoh, K.; Breedlove, B. K.; Yamashita, M. *Inorg. Chem.* **2013**, *52*, 13555−13561.

(8) Wang, H.; Qian, K.; Qi, D.; Cao, W.; Wang, K.; Gao, S.; Jiang, J. *Chem. Sci.* **2014**, *5*, 3214−3220.

DOI: 10.1021/acs.inorgchem.5b00477
Inorg. Chem. 2015, 54, 5795−5805

(9) Wang, K.; Qi, D.; Wang, H.; Cao, W.; Li, W.; Liu, T.; Duan, C.; Jiang, J. *Chem.—Eur. J.* **2013**, *19*, 11162−11166.
(10) Wang, H.; Cao, W.; Liu, T.; Duan, C.; Jiang, J. *Chem.—Eur. J.* **2013**, *19*, 2266−2270.
(11) Wang, H.; Liu, T.; Wang, K.; Duan, C.; Jiang, J. *Chem.—Eur. J.* **2012**, *18*, 7691−7694.
(12) Wang, H.; Wang, K.; Tao, J.; Jiang, J. *Chem. Commun.* **2012**, *48*, 2973−2975.
(13) Wang, H.; Qian, K.; Wang, K.; Bian, Y.; Jiang, J.; Gao, S. *Chem. Commun.* **2011**, *47*, 9624−9626.
(14) Huang, W.; Xiang, H.; Gong, Q.; Huang, Y.; Huang, C.; Jiang, J. *Chem. Phys. Lett.* **2003**, *374*, 639−644.
(15) Sheng, N.; Zhu, P.; Ma, C.; Jiang, J. *Dyes Pigm.* **2009**, *81*, 91−96.
(16) Sheng, N.; Yuan, Z.; Wang, J.; Chen, W.; Sun, J.; Bian, Y. *Dyes Pigm.* **2012**, *95*, 627−631.
(17) Wang, H.; Qi, D.; Xie, Z.; Cao, W.; Wang, K.; Shang, H.; Jiang, J. *Chem. Commun.* **2013**, *49*, 889−891.
(18) Lu, J.; Ma, P.; Zhang, X.; Jiang, J. *Dalton Trans.* **2011**, *40*, 12895−12900.
(19) Lu, G.; Chen, Y.; Zhang, Y.; Bao, M.; Bian, Y.; Li, X.; Jiang, J. *J. Am. Chem. Soc.* **2008**, *130*, 11623−11630.
(20) Bouvet, M.; Gaudillat, P.; Suisse, J.-M. *J. Porphyrins Phthalocyanines* **2013**, *17*, 628−635.
(21) Buchler, J. W.; Ng, D. K.P. In *The Porphyrin Handbook*; Kadish, K. M.; Smith, K. M.; Guilard, R., Eds.; Academic Press: San Diego, 2000; Vol. *3*, pp 245−294.
(22) Weiss, R.; Fischer, J. In *The Porphyrin Handbook*; Kadish, K. M.; Smith, K. M.; Guilard, R., Eds.; Academic Press: San Diego, 2003; Vol. *16*, pp 171−246.
(23) Bian, Y.; Zhang, Y.; Ou, Z.; Jiang, J. In *The Handbook of Porphyrin Science*; Kadish, K. M.; Smith, K. M.; Guilard, R., Eds.; World Scientific Publishing Co.: Singapore, 2011; Vol. *14*, pp 249−460.
(24) Jiang, J.; Ng, D. K. P. *Acc. Chem. Res.* **2009**, *42*, 79−88.
(25) Zhu, P.; Pan, N.; Ma, C.; Sun, X.; Arnold, D. P.; Jiang, J. *Eur. J. Inorg. Chem.* **2004**, 518−523.
(26) Sun, X.; Cui, X.; Arnold, D. P.; Choi, M. T. M.; Ng, D. K. P.; Jiang, J. *Eur. J. Inorg. Chem.* **2003**, 1555−1561.
(27) Sun, X.; Li, R.; Wang, D.; Dou, J.; Zhu, P.; Lu, F.; Ma, C.; Choi, C.-F.; Cheng, D. Y. Y.; Ng, D. K. P.; Kobayashi, N.; Jiang, J. *Eur. J. Inorg. Chem.* **2004**, 3806−3813.
(28) Gryko, D.; Li, J.; Diers, J. R.; Roth, K. M.; Bocian, D. F.; Kuhr, W. G.; Lindsey, J. S. *J. Mater. Chem.* **2001**, *11*, 1162−1180.
(29) Li, J.; Gryko, D.; Dabke, R. B.; Diers, J. R.; Bocian, D. F.; Kuhr, W. G.; Lindsey, J. S. *J. Org. Chem.* **2000**, *65*, 7379−7390.
(30) Padmaja, K.; Youngblood, W. J.; Wei, L.; Bocian, D. F.; Lindsey, J. S. *Inorg. Chem.* **2006**, *45*, 5479−5492.
(31) Gross, T.; Chevalier, F.; Lindsey, J. S. *Inorg. Chem.* **2001**, *40*, 4762−4774.
(32) Schweikart, K.-H.; Malinovskii, V. L.; Yasseri, A. A.; Li, J.; Lysenko, A. B.; Bocian, D. F.; Lindsey, J. S. *Inorg. Chem.* **2003**, *42*, 7431−7446.
(33) Lysenko, A. B.; Malinovskii, V. L.; Padmaja, K.; Wei, L.; Diers, J. R.; Bocian, D. F.; Lindsey, J. S. *J. Porphyrins Phthalocyanines* **2005**, *9*, 491−508.
(34) Tanaka, H.; Ikeda, T.; Takeuchi, M.; Sada, K.; Shinkai, S.; Kawai, T. *ACS Nano* **2011**, *5*, 9575−9582.
(35) Martynov, A. G.; Zubareva, O. V.; Gorbunova, Y. G.; Sakharov, S. G.; Nefedov, S. E.; Dolgushin, F. M.; Tsivadze, A. Y. *Eur. J. Inorg. Chem.* **2007**, 4800−4807.
(36) Birin, K. P.; Gorbunova, Y. G.; Tsivadze, A. Y. *Dalton Trans.* **2012**, *41*, 9672−9681.
(37) Lu, J.; Deng, Y.; Zhang, X.; Kobayashi, N.; Jiang, J. *Inorg. Chem.* **2011**, *50*, 2562−2567.
(38) Lei, S.; Deng, K.; Yang, Y.; Zeng, Q.; Wang, C.; Jiang, J. *Nano Lett.* **2008**, *8*, 1836−1843.
(39) Gross, Z.; Galili, N.; Saltsman, I. *Angew. Chem., Int. Ed.* **1999**, *38*, 1427−1429.
(40) Gross, Z.; Galili, N.; Simkhovich, L.; Saltsman, I.; Botoshansky, M.; Bläser, D.; Boese, R.; Goldberg, I. *Org. Lett.* **1999**, *1*, 599−602.
(41) Paolesse, R.; Mini, S.; Sagone, F.; Boschi, T.; Jaquinod, L.; Nurco, D. J.; Smith, K. M. *Chem. Commun.* **1999**, 1307−1308.
(42) Gryko, D. T. *Chem. Commun.* **2000**, 2243−2244.
(43) Paolesse, R. In *The Porphyrin Handbook*; Kadish, K. M.; Smith, K. M.; Guilard, R., Eds.; Academic Press: San Diego, 2000; Vol. *2*, pp 201−232.
(44) Erben, C.; Will, S.; Kadish, K. M. In *The Porphyrin Handbook*; Kadish, K. M.; Smith, K. M.; Guilard, R., Eds.; Academic Press: San Diego, 2000; Vol. *2*, pp 233−300.
(45) Gryko, D. T. *Eur. J. Org. Chem.* **2002**, 1735−1743.
(46) Gross, Z. *J. Biol. Inorg. Chem.* **2001**, *6*, 733−738.
(47) Paolesse, R. *Synlett* **2008**, 2215−2230.
(48) Gryko, D. T.; Fox, J. P.; Goldberg, D. P. *J. Porphyrins Phthalocyanines* **2004**, *8*, 1091−1105.
(49) Aviv-Harel, I.; Gross, Z. *Chem.—Eur. J.* **2009**, *15*, 8382−8394.
(50) Aviv, I.; Gross, Z. *Chem. Commun.* **2007**, 1987−1999.
(51) Flamigni, L.; Gryko, D. T. *Chem. Soc. Rev.* **2009**, *38*, 1635−1646.
(52) Liu, H.; Mahmood, M. H. R.; Qiu, S.; Chang, C. K. *Coord. Chem. Rev.* **2013**, *257*, 1306−1333.
(53) Aviv-Harel, I.; Gross, Z. *Coord. Chem. Rev.* **2011**, *255*, 717−736.
(54) Lu, G.; Yan, S.; Shi, M.; Yu, W.; Li, J.; Zhu, W.; Ou, Z.; Kadish, K. M. *Chem. Commun.* **2015**, *51*, 2411−2413.
(55) Pan, N.; Jiang, J.; Cui, X.; Arnold, D. P. *J. Porphyrins Phthalocyanines* **2002**, *6*, 347−357.
(56) Chabach, D.; De Cian, A.; Fischer, J.; Weiss, R.; Bibout, M. E. M. *Angew. Chem., Int. Ed. Engl.* **1996**, *35*, 898−899.
(57) Bai, M.; Bao, M.; Ma, C.; Arnold, D. P.; Choi, M. T. M.; Ng, D. K. P.; Jiang, J. *J. Mater. Chem.* **2003**, *13*, 1333−1339.
(58) Moussavi, M.; De Cian, A.; Fischer, J.; Weiss, R. *Inorg. Chem.* **1986**, *25*, 2107−2108.
(59) Bian, Y.; Wang, R.; Jiang, J.; Lee, C.-H.; Wang, J.; Ng, D. K. P. *Chem. Commun.* **2003**, 1194−1195.
(60) Lu, F.; Sun, X.; Li, R.; Liang, D.; Zhu, P.; Choi, C.-F.; Ng, D. K. P.; Fukuda, T.; Kobayashi, N.; Bai, M.; Ma, C.; Jiang, J. *New J. Chem.* **2004**, *28*, 1116−1122.
(61) Chen, Y.; Liu, H.; Zhu, P.; Zhang, Y.; Wang, X.; Li, X.; Jiang, J. *Langmuir* **2005**, *21*, 11289−11295.
(62) Stites, J. G.; McCarty, C. N.; Quill, L. L. *J. Am. Chem. Soc.* **1948**, *70*, 3142−3143.
(63) Koszarna, B.; Gryko, D. T. *J. Org. Chem.* **2006**, *71*, 3707−3717.
(64) Shen, J.; Ou, Z.; Shao, J.; Galezowski, M.; Gryko, D. T.; Kadish, K. M. *J. Porphyrins Phthalocyanines* **2007**, *11*, 269−276.
(65) Pushkarev, V. E.; Breusova, M. O.; Shulishov, E. V.; Tomilov, Y. V. *Russ. Chem. Bull.* **2005**, *54*, 2087−2093.
(66) Gao, Y.; Li, R.; Dong, S.; Bian, Y.; Jiang, J. *Dalton Trans.* **2010**, *39*, 1321−1327.
(67) Spyroulias, G. A.; Coutsolelos, A. G. *Inorg. Chem.* **1996**, *35*, 1382−1385.
(68) Spyroulias, G. A.; Raptopoulou, C. P.; de Montauzon, D.; Mari, A.; Poilblanc, R.; Terzis, A.; Coutsolelos, A. G. *Inorg. Chem.* **1999**, *38*, 1683−1696.
(69) Spyroulias, G. A.; Coutsolelos, A. G.; Raptopoulou, C. P.; Terzis, A. *Inorg. Chem.* **1995**, *34*, 2476−2479.
(70) Lv, W.; Zhu, P.; Bian, Y.; Ma, C.; Zhang, X.; Jiang, J. *Inorg. Chem.* **2010**, *49*, 6628−6635.
(71) Wang, R.; Li, R.; Li, Y.; Zhang, X.; Zhu, P.; Lo, P.-C.; Ng, D. K. P.; Pan, N.; Ma, C.; Kobayashi, N.; Jiang, J. *Chem.—Eur. J.* **2006**, *12*, 1475−1485.
(72) Buchler, J. W.; Scharbert, B. *J. Am. Chem. Soc.* **1988**, *110*, 4272−4276.
(73) Bao, M.; Pan, N.; Ma, C.; Arnold, D. P.; Jiang, J. *Vib. Spectrosc.* **2003**, *32*, 175−184.
(74) Jiang, J.; Bao, M.; Rintoul, L.; Arnold, D. P. *Coord. Chem. Rev.* **2006**, *250*, 424−448.
(75) Lu, F.; Bao, M.; Ma, C.; Zhang, X.; Arnold, D. P.; Jiang, J. *Spectrochim. Acta, Part A* **2003**, *59A*, 3273−3286.

DOI: 10.1021/acs.inorgchem.5b00477
Inorg. Chem. 2015, 54, 5795−5805

(76) Zhang, Y.; Jiang, W.; Jiang, J.; Xue, Q. *J. Porphyrins Phthalocyanines* **2007**, *11*, 100−108.
(77) Zhu, P.; Lu, F.; Pan, N.; Arnold, D. P.; Zhang, S.; Jiang, J. *Eur. J. Inorg. Chem.* **2004**, 510−517.

DOI: 10.1021/acs.inorgchem.5b00477
Inorg. Chem. 2015, 54, 5795−5805